AIAA Journal
Vol. 46, No. 5, May 2008

Engineering Notes

ENGINEERING NOTES are short manuscripts describing new developments or important results of a preliminary nature. These Notes should not exceed 2500 words (where a figure or table counts as 200 words). Following informal review by the Editors, they may be published within a few months of the date of receipt. Style requirements are the same as for regular contributions (see inside back cover).

Stress-Based Optimization Method for Reproducing In-Flight Loads Using Concentrated Forces

Charbel Bou-Mosleh* and Charbel Farhat†
Stanford University,
Stanford, California 94305-3035

DOI: 10.2514/1.28668

I. Introduction

THIS Note describes an optimization algorithm for replicating a desired stress state of an aeroelastic structure using a few concentrated forces. It has potential applications, for example, in live-fire testing (LFT) [1], where it could be used to replicate a wing's in-flight loads by reproducing, on the ground, the true stress state of the wing in flight. The true stress state can be predicted using a validated, state-of-the-art, computational fluid dynamics (CFD)-based aeroelastic simulation tool such as AERO [2,3]. Then, the structure can be loaded with a few controlled concentrated forces as dictated by the algorithm to reproduce as accurately as possible the computed stress state.

Most of the related work reported in the literature is based on pure displacement or shape control of structures using smart material actuators [4–14]. Two recently proposed algorithms, however, include slope or stress as a fine-tuning criterion of an otherwise displacement-based control procedure. Indeed, Chee et al. [15] introduced a slope-displacement based algorithm, the perturbation buildup voltage distribution (PBVD), in which slope control is used to reduce the bumpiness caused by a pure displacement-based shape control technique. Also, Chen et al. [16] introduced stress control as a means of fine-tuning global displacement control. In this case, the bumpiness is reduced by minimizing the large stresses that occur at the local level. In contrast, the approach proposed in this Note focuses directly on stress control and minimizes a relative global error between the target stress state predicted by numerical simulations and the stress state generated by loading the structure with a few external forces.

II. Problem Setup and Mathematical Formulation

The success of the methodology described in this Note, particularly for LFT applications, hinges on the availability of a reliable simulation tool for accurately predicting the true stress state of the structure. Recent advances in computational mechanics, in general, and CFD-based aeroelastic computations, in particular, are such that this is possible nowadays. In this work, the aeroelastic code AERO [2,3] is used for this purpose. To reproduce the predicted stress state, embedding actuators based on smart materials in a wing structure were considered in preliminary studies [17,18] but did not lead to a feasible and successful loading method. For this reason, loading with external concentrated forces only is considered in this Note.

Consider the case of an aeroelastic wing. The approach discussed in this Note can be summarized as follows. Given a wing structure and a specific flight condition, appropriate computational fluid and finite element (FE) structural models are constructed. First, the stress state is predicted by a CFD-based aeroelastic simulation. Next, the wing structure is loaded with a feasible number of concentrated forces to reproduce the computed stress state. To determine the gain in magnitude of the forces, another computation is performed to minimize the following relative global error:

$$E_g = \frac{\|\mathbf{s} - \bar{\mathbf{s}}\|_2}{\|\bar{\mathbf{s}}\|_2} \tag{1}$$

where $\bar{\mathbf{s}}$ = target stress state predicted by an aeroelastic numerical computation and $\mathbf{s}$ = stress state induced by loading with the concentrated forces.

From Eq. (1), it follows that the crux of the proposed loading methodology consists of solving the following optimization problem:

$$\min \|\mathbf{s} - \bar{\mathbf{s}}\|_2 \tag{2}$$

Next, this optimization problem is formulated in detail and related to the parameters of the loading methodology.

Let g_i denote the gain in magnitude of the ith concentrated force with respect to a reference force, and let $\mathbf{u}_i$ denote the displacement vector of the global structure induced by a unit value of g_i. Under the reasonable linear assumption of the behavior of the structure, the total displacement of the structure when N forces are applied is

$$\mathbf{u} = \sum_{i=1}^{i=N} \mathbf{u}_i g_i = \mathbf{U}\mathbf{g} \tag{3}$$

where $\mathbf{U}$ is the matrix of displacement vectors $\mathbf{u}_i$ and $\mathbf{g}$ is the vector of gains g_i.

From Eq. (3), it follows that if $\mathbf{s}_i$ denotes the stress tensor associated with $\mathbf{u}_i$, the stress state of the wing is given by

$$\mathbf{s} = \sum_{i=1}^{i=N} \mathbf{s}_i g_i = \mathbf{S}\mathbf{g} \tag{4}$$

where $\mathbf{S}$ is the matrix of stress tensors $\mathbf{s}_i$ associated with the gains g_i.

Then, the objective is to find the gain vector $\mathbf{g}$ for which $\mathbf{s} = \bar{\mathbf{s}}$, that is, to solve

$$\mathbf{S}\mathbf{g} = \bar{\mathbf{s}} \tag{5}$$

Unfortunately, Eq. (5) can be exactly satisfied only when the total number of concentrated forces is equal to the number of degrees of freedom of the FE model of the structure, which can be quite large,

Received 1 November 2006; accepted for publication 6 January 2008.

*Post-Doctoral Scholar, Department of Mechanical Engineering, Building 500, 488 Escondido Mall.

†Professor, Department of Mechanical Engineering, Institute for Computational and Mathematical Engineering, and Department of Aeronautics and Astronautics (by courtesy), Building 500, 488 Escondido Mall. Fellow AIAA.

and/or $\bar{\mathbf{s}}$ is in the range of the matrix $\mathbf{S}$, which can be written as $\bar{\mathbf{s}} \in R(\mathbf{S})$. Hence, a nonzero residual

$$\mathbf{r} = \mathbf{S}\mathbf{g} - \bar{\mathbf{s}} \tag{6}$$

is to be expected and accepted. Therefore, the objective becomes to minimize an adequate norm of the above residual, for example, its two-norm (Euclidean norm). Because some concentrated force application points and orientations, referred to collectively here and in the remainder of this Note as positions, can be expected to contribute better than others at reproducing the in-flight loads, $\|\mathbf{S}\mathbf{g} - \bar{\mathbf{s}}\|_2$ should be minimized in principle over all of the gains, positions, and number of concentrated forces.

In summary, the proposed stress-control-based loading methodology is governed by a mathematical problem of the form

$$\min_{\substack{N \in \mathbb{R} \\ \mathbf{g} \in \mathbb{R}^N \\ \mathbf{X} \in \mathbb{R}^{3\times N}}} \|\mathbf{S}(\mathbf{X})\mathbf{g} - \bar{\mathbf{s}}\|_2 \qquad \mathbf{C}(\mathbf{g}) \leq 0 \tag{7}$$

where $\mathbf{X}$ denotes the position vector of the concentrated forces and $\mathbf{C}(\mathbf{g})$ is a matrix of constraints specifying, for example, an acceptable number of forces not to exceed N_a and the maximum allowable stress in each structural member as a percentage of the yield stress.

In practice, a range for N_a is set by practical considerations. Furthermore, a reasonably good position of the concentrated forces can be determined by a simple iterative procedure and good engineering judgment. This is discussed in Sec. III.B and illustrated in Secs. IV.A and IV.B of this Note. Therefore, for all practical purposes, the governing problem simplifies to

$$\min_{\mathbf{g} \in \mathbb{R}^N} \|\mathbf{S}\mathbf{g} - \bar{\mathbf{s}}\|_2 \qquad \mathbf{C}(\mathbf{g}) \leq 0 \tag{8}$$

III. Solution Approach

A realistic but larger than otherwise number of concentrated forces increases the complexity of the loading methodology when used in real-life applications. On the other hand, Eq. (7) highlights the fact that a larger than otherwise number of concentrated forces decreases the relative global error E_g [Eq. (1)]. Hence, the maximum acceptable number of concentrated forces, N_a, is set in the form of an acceptable range by considering a compromise between minimizing the complexity of the application and maximizing its accuracy.

To determine the position of the concentrated forces, the following property of the mathematical problem formulated in Sec. II is first established: Given a wing, a corresponding FE structural model, and a configuration of concentrated forces defined by their number N and their positions, the smallest achievable relative global error (1) can be evaluated a priori. Then, this property is exploited to determine N_a and a good orientation of the concentrated forces. The points of application of these forces are determined by an iterative procedure described in Sec. III.B.

A. A Priori Prediction of Performance of a Given Configuration of Concentrated Forces

From the definition of N_a and Eq. (7), it follows that the relative global error (1) is smaller for $N = N_a$ than for any value of the number of concentrated forces $N < N_a$. Assume for now that N_a is set by test considerations only.

Let $\mathbf{S}_a$ denote the matrix of the stress tensors $\mathbf{s}_i$ obtained by loading the wing structure with N_a concentrated forces and let $\mathbf{R}_a$ denotes its range. $\mathbf{R}_a$ can be determined a priori from the singular value decomposition (SVD) [19,20]

$$\mathbf{S}_a = \mathbf{U}_a \boldsymbol{\Sigma}_a \mathbf{V}_a^T \tag{9}$$

which shows that $\mathbf{R}_a$ is the span of the first r columns of $\mathbf{U}_a$, where r is the number of nonzero singular values in the diagonal matrix $\boldsymbol{\Sigma}_a$.

If $\bar{\mathbf{s}} \in R(\mathbf{S}_a)$, the solution of problem (8) formulated with $\mathbf{S} = \mathbf{S_a}$ guarantees in theory a zero relative global error (1) and therefore a perfect reproduction of the stress state.

On the other hand, if $\bar{\mathbf{s}} \notin R(\mathbf{S}_a)$, $\bar{\mathbf{s}}$ can be decomposed as

$$\bar{\mathbf{s}} = \bar{\mathbf{s}}_1 + \bar{\mathbf{s}}_2 \tag{10}$$

where

$$\begin{cases} \bar{\mathbf{s}}_1 \in R(\mathbf{S}_a) \\ \bar{\mathbf{s}}_2 \in Ker\left(\mathbf{S}_a^T\right) \end{cases}$$

The superscript T denotes the transpose operation and Ker the null space. From Eq. (9), it follows that a basis of $Ker(\mathbf{S}_a^T)$, $\mathbf{N}_a$, is given by the last $n - r$ columns of the matrix $\mathbf{U}_a$, where n denotes the number of rows of the matrix $\mathbf{S}_a$. Hence, the matrix $\mathbf{N}_a$ can also be computed a priori from the SVD (9). From Eqs. (9) and (10), and the previous observations, it follows that

1) $\bar{\mathbf{s}}$ can be written as

$$\bar{\mathbf{s}} = \bar{\mathbf{s}}_1 + \mathbf{N}_a \mathbf{v} \tag{11}$$

where $\mathbf{v}$ remains to be determined. Multiplying Eq. (11) by $\mathbf{N}_a^T$ gives

$$\mathbf{N}_a^T \bar{\mathbf{s}} = \mathbf{N}_a^T \bar{\mathbf{s}}_1 + \mathbf{N}_a^T \mathbf{N}_a \mathbf{v} \tag{12}$$

Since $\bar{\mathbf{s}}_1 \in R(\mathbf{S}_a)$, then

$$\mathbf{N}_a^T \bar{\mathbf{s}}_1 = \mathbf{0} \tag{13}$$

and therefore

$$\mathbf{N}_a^T \bar{\mathbf{s}} = \mathbf{N}_a^T \mathbf{N}_a \mathbf{v} \longrightarrow \mathbf{v} = \left(\mathbf{N}_a^T \mathbf{N}_a\right)^{-1} \mathbf{N}_a^T \bar{\mathbf{s}} \tag{14}$$

Substituting Eq. (14) into Eq. (11) gives

$$\bar{\mathbf{s}} = \bar{\mathbf{s}}_1 + \mathbf{N}_a\left(\mathbf{N}_a^T \mathbf{N}_a\right)^{-1} \mathbf{N}_a^T \bar{\mathbf{s}} \longrightarrow \bar{\mathbf{s}}_1 = \left(\mathbf{I} - \mathbf{N}_a\left(\mathbf{N}_a^T \mathbf{N}_a\right)^{-1} \mathbf{N}_a^T\right)\bar{\mathbf{s}} \tag{15}$$

2) $\bar{\mathbf{s}}_2$ can be expressed as

$$\bar{\mathbf{s}}_2 = \bar{\mathbf{s}} - \bar{\mathbf{s}}_1 \longrightarrow \bar{\mathbf{s}}_2 = \mathbf{N}_a\left(\mathbf{N}_a^T \mathbf{N}_a\right)^{-1} \mathbf{N}_a^T \bar{\mathbf{s}} \tag{16}$$

3) There exists a vector $\mathbf{g}$ such that

$$\mathbf{S}_a \mathbf{g} = \bar{\mathbf{s}}_1 \tag{17}$$

4) The smallest possible relative global error (1) achievable by the proposed loading methodology is

$$E_g = \frac{\|\mathbf{S}_a \mathbf{g} - \bar{\mathbf{s}}\|_2}{\|\bar{\mathbf{s}}\|_2} = \frac{\|\mathbf{S}_a \mathbf{g} - \bar{\mathbf{s}}_1 - \bar{\mathbf{s}}_2\|_2}{\|\bar{\mathbf{s}}\|_2} = \frac{\|\bar{\mathbf{s}}_2\|_2}{\|\bar{\mathbf{s}}\|_2} = \frac{\left\|\mathbf{N}_a\left(\mathbf{N}_a^T \mathbf{N}_a\right)^{-1} \mathbf{N}_a^T \bar{\mathbf{s}}\right\|_2}{\|\bar{\mathbf{s}}\|_2} \tag{18}$$

Equation (18) reveals that it is possible to calculate the relative global error of the stress state achieved by the proposed loading methodology without solving for the actual gains in the concentrated forces. If this relative global error (18) is below a specified maximum acceptable relative global error, E_{g_a}, one can proceed and compute the solution of the minimization problem (8) analytically as follows:

$$\mathbf{g} = \mathbf{V}_a \boldsymbol{\Sigma}_a^+ \mathbf{U}_a^T \left(\mathbf{I} - \mathbf{N}_a\left(\mathbf{N}_a^T \mathbf{N}_a\right)^{-1} \mathbf{N}_a^T\right)\bar{\mathbf{s}} \tag{19}$$

where $\mathbf{U}_a$, $\boldsymbol{\Sigma}_a$, and $\mathbf{V}_a$ are the SVD factors of the matrix $\mathbf{S}_a$. In this case, one can also recursively consider loading the structure with fewer concentrated forces ($N < N_a$), until the relative global error

$$E_g = \frac{\|\mathbf{N}(\mathbf{N}^T\mathbf{N})^{-1}\mathbf{N}^T \bar{\mathbf{s}}\|_2}{\|\bar{\mathbf{s}}\|_2} \tag{20}$$

exceeds the maximum acceptable relative global error, E_{g_a}, at which point the previous number of concentrated forces is adopted and the gain vector is given by

$$\mathbf{g} = \mathbf{V}\mathbf{\Sigma}^{+}\mathbf{U}^{T}(\mathbf{I} - \mathbf{N}(\mathbf{N}^{T}\mathbf{N})^{-1}\mathbf{N}^{T})\bar{\mathbf{s}} \tag{21}$$

On the other hand, if the relative global error (18) is unacceptable ($E_g > E_{g_a}$), it can be automatically concluded that the structure cannot be put in the desired stress state $\bar{\mathbf{s}}$ with the desired precision using the N_a controllable concentrated forces. In this case, a different position of the forces should be tried or increasing the number of forces should be considered.

B. Finding Positions of Concentrated Forces

The following iterative "reduction" procedure can be applied for finding a good position of the N_a concentrated forces.

First, the hypothetical scenario of a massive loading ($N \gg N_a$) is analyzed, but not considered for practical application. An orientation is chosen for each concentrated force using good engineering judgement. For example, each force is normal to the surface of the wing at the point of application. This defines the "initial configuration" of the concentrated forces. After the initial gains are computed to minimize the relative global error E_g (1), all forces with a gain below a specified percentage of the largest gain are discarded. This analysis cycle is recursively repeated while requiring $E_g < E_{g_a}$, until the number of forces is reduced to a value within the specified range for N_a. During the iterations, the orientation of the forces can be kept unchanged unless required for reducing N without violating the constraint $E_g < E_{g_a}$.

As shown in Sec. IV, the reduction procedure described previously converges rapidly.

IV. Simulated Applications to Slender and Cropped Delta Wings

In this section, the proposed loading methodology is illustrated, and its potential is evaluated, with its application to a slender wing (the ARW2 wing) and a cropped delta wing (the F-16 Block 40 wing). In the case of the ARW2 wing, the transonic flight conditions defined by the Mach number $M_\infty = 0.8$, the altitude $H = 40,000$ ft, and the trim angle of attack $\alpha = 2.5$ deg are considered. In the case of the F-16 Block 40 wing, these are set to $M_\infty = 0.8$, $H = 10,000$ ft, and $\alpha = 2.5$ deg. For each wing, a reasonably well-resolved FE structural model and a CFD grid suitable for inviscid (Euler) flow computations are constructed.

For both examples, it is assumed that $5 \leq N_a \leq 10$ and $E_g \approx 10\%$ are reasonable range values. For simplicity, it is also assumed that the forces are normal to the surface of the wing at the point of application.

A. ARW-2 Wing

The aeroelastic research wing (ARW-2) was developed at the NASA Langley Research Center for unsteady pressure testing in the Langley Transonic Dynamics Tunnel. This wing has an aspect ratio of 10.3, a leading-edge sweepback angle of 28.8 deg, and a supercritical airfoil [21]. It is represented here by a detailed FE model that accounts for its spars, ribs, skin, hinges, and control surfaces. This model is composed of 456 nodes, 1151 shell elements, 180 beam elements, 434 bar elements, and several discrete masses. After it is clamped at its root, this FE model has 2700 active degrees of freedom (Fig. 1).

The initial value of N is set to 380. The SVD analysis of the initial value of the matrix $\mathbf{S}$ reveals that its range does not contain the numerically predicted stress state. Nevertheless, the solution of the minimization problem (8) delivers gains that yield a relative global error that is as small as 6.4%. This result indicates that even though it is not exactly in the range of the concentrated forces, the predicted in-flight stress state can be reproduced fairly accurately by the proposed loading methodology when the considered number of forces is very large. Next, the reduction strategy outlined in Sec. III.B is applied to reduce the number of concentrated forces to a value within the range of N_a. After the initial iteration, all forces with a gain smaller than 10% of the largest gains are eliminated. Amazingly, this reduces the number of forces to 20 while delivering a stress state with a relative global error of 7.8%. Using these 20 forces, the minimization problem (8) is solved again and the forces with a gain smaller than 10% of the largest gain are eliminated. This reduces the number of forces to 11 and increases only slightly the value of the relative global error to $E_g = 8.6\%$. A third reduction cycle leads to the five forces configuration shown in Fig. 2 whose gains reproduce the predicted in-flight stress state with a relative global error of 10.2% only.

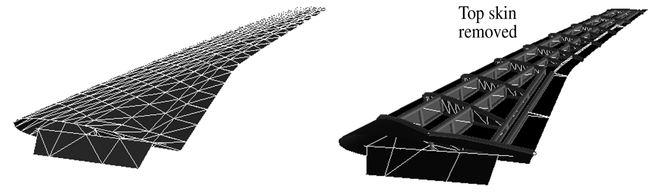

Fig. 1 Detailed FE model of the ARW-2 wing.

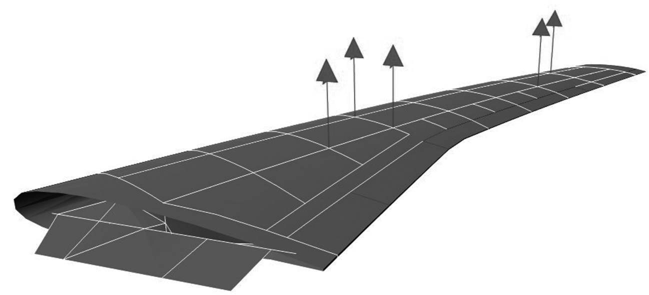

Fig. 2 Loading of the ARW-2 wing (five concentrated forces).

B. F-16 Block 40 Wing

The half-span of the F-16 Block 40 wing is equal to 130 in. and its mean chord length is equal to 96 in. This wing with its spars, ribs, skin, hinges, and control surfaces is represented here by a detailed FE model with 9131 nodes, 2835 bar elements, 800 beam elements, a large number of spring, shell, and solid elements, and 36,926 active degrees of freedom after it is clamped at its root (see Fig. 3).

Starting from a hypothetical massive loading with 407 external forces applied as in the case of the ARW2 wing, the in-flight stress state predicted by a CFD-based aeroelastic simulation is reproduced with a relative global error of 5.7%. Next, applying the reduction procedure described in Sec. III.B, the number of forces is reduced in

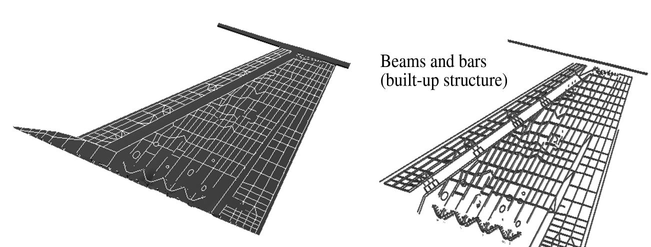

Fig. 3 Detailed finite element model of the F16 wing Block 40.

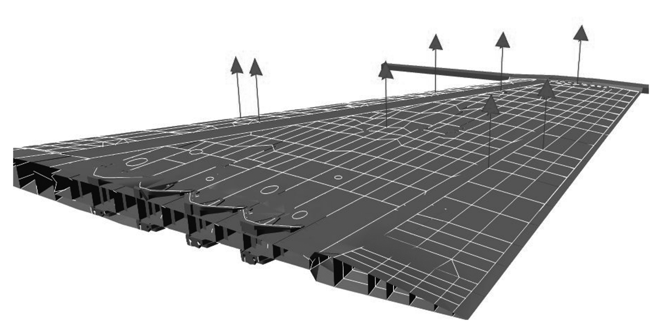

Fig. 4 Loading of the F-16 Block 40 wing (eight forces).

Table 1 Reduction of the number of external forces and effect on accuracy (F-16 Block 40 wing)

No. of concentrated forces (N)	Relative global error (E_g)
407	5.7%
59	9.3%
39	9.8%
17	11.1%
8	11.7%

four iterations to eight forces. The number of forces obtained at each iteration and the corresponding accuracy of the loading methodology are summarized in Table 1.

Using eight external forces (Fig. 4), the proposed loading methodology reproduces the predicted in-flight stress state of the F-16 Block 40 wing with a relative global error of 11.7% and without causing any structural member of the wing to yield.

V. Conclusions

The loading methodology described in this Note is capable of replicating a desired stress state of a structure using a few external concentrated forces. The desired stress state of this structure is numerically predicted, and a few external concentrated forces are applied to reproduce it. Simulation results for the ARW2 wing and the F-16 Block 40 wing reveal that with five to eight concentrated forces, the proposed loading methodology is capable of reproducing the simulated in-flight stress states with a relative global error of the order of 10–12%. This suggests a good potential for real applications.

References

[1] National Research Council (NRC), Committee on Weapons Effect on Airborne Systems, *Vulnerability Assessment of Aircraft: A Review of the Department of Defense Live Fire Test and Evaluation Program*, National Academy Press, Washington, D.C., 1993.

[2] Farhat, C., Geuzaine, P., and Brown, G., "Application of a Three-Field Nonlinear Fluid-Structure Formulation to the Prediction of the Aeroelastic Parameters of an F-16 Fighter," *Computers and Fluids*, Vol. 32, No. 1, Jan. 2003, pp. 3–29. doi:10.1016/S0045-7930(01)00104-9

[3] Geuzaine, P., Brown, G., Harris, C., and Farhat, C., "Aeroelastic Dynamic Analysis of a Full F-16 Configuration for Various Flight Conditions," *AIAA Journal*, Vol. 41, No. 3, 2003, pp. 363–371.

[4] Austin, F., Rossi, M. J., Jameson, A., Van Nostrand, W., Su, J., and Knowles, G., "Active Rib Experiment for Adaptive Conformal Wing," *Third International Conference on Adaptive Structures*, Technomic Publishing Co., Inc., Lancaster, PA, Nov. 1992, pp. 43–55.

[5] Bruno, R., Salama, M., and Garba, J., "Actuator Placement for Static Shape Control of Nonlinear Truss Structure," *Third International Conference on Adaptive Structures*, Technomic Publishing Co., Inc., Lancaster, PA, Nov. 1992, pp. 433–445.

[6] Mikulas, M. M., Jr., Wada, B. K., Farhat, C., Thorwald, G., and Withnell, P., "Initially Deformed Truss Geometry for Improving the Adaptive Performance of Truss Structures," *Third International Conference on Adaptive Structures*, Technomic Publishing Co., Inc., Lancaster, PA, Nov. 1992, pp. 305–319.

[7] Khot, N. S., Appa, K., Ausman, J., and Eastep, F. E., "Deformation of a Flexible Wing Using an Actuating System for a Rolling Maneuver Without Ailerons," *39th AIAA/ASME/ASCE/AHS/ASC Structures, Structural Dynamics, and Materials Conference*, AIAA, Reston, VA, April 1998, pp. 876–884; also AIAA Paper 98-1802, 1998.

[8] Khot, N. S., Zweber, J. V., Veley, D. E., Appa, K., and Eastep, F. E., "Optimization of a Flexible Composite Wing for Pull-Up Maneuver with Internal Actuation," *42nd AIAA/ASME/ASCE/AHS/ASC Structures, Structural Dynamics, and Materials Conference*, AIAA, Reston, VA, April 2001; also AIAA Paper 2001-1274, 2001.

[9] Kudva, J. N., Appa, K., Van Way, C. B., and Lockyer, A. J., "Adaptive Smart Wing Design for Military Aircraft: Requirements, Concepts and Payoffs," *SPIE Smart Structures and Materials 1995: Industrial and Commercial Applications of Smart Structures Technologies*, Vol. 2447, SPIE–International Society for Optical Engineering, Bellingham, WA, 1995, pp. 35–44. doi:10.1117/12.209347.

[10] Maute, K., and Reich, G., "An Aeroelastic Topology Optimization Approach for Adaptive Wing Design," *45th AIAA/ASME/ASCE/AHS/ASC Structures, Structural Dynamics, and Materials Conference*, AIAA, Reston, VA, April 2004; also AIAA Paper 2004-1805, 2004.

[11] Sarjeant, R. A., Frecker, M., and Gandhi, F. S., "Optimal Design of a Smart Conformable Rotor Airfoil," *Proceedings of IMECE2002, ASME International Mechanical Engineering Congress & Exposition*, ASME, Fairfield, NJ, Nov. 2002, pp. 249–259; also ASME Paper IMECE2002-39030.

[12] Haftka, R. T., and Adelman, H. M., "An Analytical Investigation of Shape Control of Large Space Structures by Applied Temperatures," *AIAA Journal*, Vol. 23, No. 3, 1985, pp. 450–457.

[13] Haftka, R. T., "Limits on Static Shape Control for Space Structures," *AIAA Journal*, Vol. 29, No. 11, 1991, pp. 1945–1950.

[14] Burdisso, R. A., and Haftka, R. T., "Optimal Location of Actuators for Correcting Distortions in Large Truss Structures," *AIAA Journal*, Vol. 27, No. 10, 1989, pp. 1406–1411.

[15] Chee, C., Tong, L., and Steven, G. P., "Static Shape Control of Composite Plates Using a Slope-Displacement Based Algorithm," *AIAA Journal*, Vol. 40, No. 8, Aug. 2002, pp. 1611–1618.

[16] Chen, W., Wang, D., and Li, M., "Static Shape Control Employing Displacement-Stress Dual Criteria," *Smart Materials and Structures*, Vol. 13, No. 3, June 2004, pp. 468–472. doi:10.1088/0964-1726/13/3/003

[17] Bou-Mosleh, C., Farhat, C., and Maute, K., "A Stress-Control-Based Live-Fire Ground Testing Methology," *45st AIAA/ASME/ASCE/AHS/ASC Structures, Structural Dynamics, and Materials Conference*, AIAA, Reston, VA, April 2004; also AIAA Paper 2004-1540.

[18] Bou-Mosleh, C., "Methodologies for Reproducing In-Flight Loads of Aircraft Wings on the Ground and Predicting Their Response to Battle-Induced Damage," Ph.D. Thesis, University of Colorado, Boulder, CO, Dec. 2005.

[19] Golub, G., and Loan, C. V., *Matrix Computations*, The Johns Hopkins University, Baltimore, MD, 1983.

[20] Watkins, D., *Fundamentals of Matrix Computations*, Wiley, New York, 2002.

[21] Sandford, M., Seidel, D., Eckstrom, C. V., and Spain, C. V., "Geometric and Structural Properties of an Aeroelastic Research Wing (ARW-2)," NASA TM 4110, April 1989.

E. Livne
Associate Editor